

# Enhanced quantum entanglement in the non-Markovian dynamics of biomolecular excitons

M. Thorwart<sup>a,b</sup>, J. Eckel<sup>b</sup>, J.H. Reina<sup>c</sup>, P. Nalbach<sup>a</sup>, S. Weiss<sup>b,d</sup>

<sup>a</sup>*Freiburg Institute for Advanced Studies (FRIAS), Universität Freiburg, 79104 Freiburg, Germany*

<sup>b</sup>*Institut für Theoretische Physik, Heinrich-Heine-Universität Düsseldorf, 40225 Düsseldorf, Germany*

<sup>c</sup>*Departamento de Física, Universidad del Valle, A.A. 25360, Cali, Colombia*

<sup>d</sup>*Niels-Bohr-Institute, Universitetsparken 5, 2100 Copenhagen, Denmark*

---

## Abstract

We show that quantum coherence of biomolecular excitons is maintained over exceedingly long times due to the constructive role of their non-Markovian protein-solvent environment. Using a numerically exact approach, we demonstrate that a slow quantum bath helps to sustain quantum entanglement of two pairs of Förster coupled excitons, in contrast to a Markovian environment. We consider the crossover from a fast to a slow bath and from weak to strong dissipation and show that a slow bath can generate robust entanglement. This persists to surprisingly high temperatures, even higher than the excitonic gap and is absent for a Markovian bath.

*Key words:* Quantum entanglement in biomolecules, open quantum systems, Förster energy transfer in excitonic systems

---

## 1. Introduction

Quantum coherent dynamics at the initial stages of photosynthesis in complex biomolecular structures seems to promote the efficiency of energy transfer from the light-harvesting antenna complexes to the chemical reaction centers [1, 2, 3, 4]. This hypothesis has recently been boosted by experiments revealing long-lived quantum coherent excitonic dynamics in the energy transfer among bacteriochlorophyll complexes over a surprisingly long time of around 600 fs measured at 77 K [1]. In addition, electronic coherences between excited states in purple photosynthetic bacteria have been monitored

in a two-color photon echo experiment [2]. Both works lead to the conclusion that the collective long-range electrostatic response of the biomolecular protein environment to the electronic excitations should be responsible for the long-lived quantum coherence. Furthermore, the obtained time scales [2] for the short-time dynamics of the nuclear modes coupled to the excitonic states of two chromophores are almost identical. This points to the special and constructive role of the quantum environment for the photoexcitations. The often assumed coupling of the chromophores to fast and independent quantum baths does not hold in this case. In fact, the two chromophores are embedded in the *same* protein-solvent environment. These results corroborate experimental studies [3] which show that energy transport sensitively depends on the spatial properties of the delocalized excited-state wave functions of the *whole* pigment-protein complex. In addition, there are reports of coherently controlled wave packet quantum dynamics artificially generated by laser pulses in the light-harvesting antenna of the bacteria *Rhodospseudomonas acidophila* [4].

An appropriate theoretical description of the biomolecular quantum dynamics has to account for the environmental time scales typically being of the same order of magnitude as the excitonic time scales [5]. This fact renders the dynamics highly non-Markovian and rather elaborate techniques are required to address the entire cross-over from fast to slowly responding baths.

Here, we perform a deterministic evaluation of real-time path integrals [6, 7, 8] where all non-Markovian effects are exactly included. We provide numerically exact results for the quantum coherent dynamics of photoexcitations in coupled chromophores, where the time evolution of the protein-solvent bath happens on time scales comparable to the exciton dynamics. We show that the non-Markovian effects help to sustain quantum coherence over rather long times. Furthermore, quantum entanglement of two chromophore pairs is shown to be more stable under the influence of a non-Markovian bath. Even at high temperatures, a slow bath can generate considerable entanglement, a feature absent in the Markovian case. We mention that recently, quantum entanglement of two optical two-level systems coupled to a common localized environmental mode has been studied beyond the Markov approximation at zero temperature [9].

## 2. Model for a single chromophore pair

A single chromophore (index  $i$ ) is modeled as a quantum two level system described by Pauli matrices  $\tau_{x,y,z}^i$  with energy gap  $E_i$  between ground-state  $|g_i\rangle$  and excited state  $|e_i\rangle$  [5]. The protein-solvent environment is formalized as a harmonic bath yielding the standard spin-boson Hamiltonian for each chromophore [5]. The Förster coupling between two chromophores is given by  $H_{12} = \frac{\hbar\Delta}{2}(\tau_x^1\tau_x^2 + \tau_y^1\tau_y^2)$  [5]. Observing that the fluorescence lifetime of the chromophores is much larger than all other time scales, we may neglect the radiative decay [5]. Then, the system's total number of excitations is a constant of motion, and the two-chromophore system can be reduced to a single spin-boson model of one chromophore pair (with the Pauli matrices  $\sigma_{x,z}$ ):

$$H_1 = \frac{\hbar\epsilon}{2}\sigma_z + \frac{\hbar\Delta}{2}\sigma_x + \hbar\sigma_z \sum_{\kappa} \lambda_{\kappa}(b_{\kappa}^{\dagger} + b_{\kappa}) + \sum_{\kappa} \hbar\omega_{\kappa}b_{\kappa}^{\dagger}b_{\kappa}, \quad (1)$$

where  $\epsilon = E_1 - E_2$ , and  $b_{\kappa}$  describe bosonic bath operators with couplings  $\lambda_{\kappa}$ . We consider equal chromophores  $E_1 = E_2$ ; the effective basis for a chromophore pair is given by  $\{|\uparrow\rangle = |e_1g_2\rangle, |\downarrow\rangle = |g_1e_2\rangle\}$ .

The spectral density [10] follows from a microscopic derivation [11]. Different forms of a Debye dielectric can be assumed, but in any case, lead to an Ohmic form,  $G(\omega) = 2\pi\alpha\omega e^{-\omega/\omega_c}$ . The dimensionless damping constant  $\alpha$  of the protein-solvent can be related to the parameters of the dielectric model [11]. One finds for the order of magnitude of  $\alpha \sim 0.01 - 0.1$  [5, 11]. We use an exponential form of the cut-off at frequency  $\omega_c$ . This sets the time-scale for the bath dynamics and is related to the reorganization energy  $E_r \sim 2\alpha\hbar\omega_c$ . If  $\Delta \ll \omega_c$  and  $\alpha \ll 1$ , the bath evolves fast compared to the system and loses its memory quickly, rendering a Markovian approximation and the standard Bloch-Redfield description [12] suitable. This situation is ubiquitous in many physical systems, e.g., ion traps, quantum dots, and superconducting devices [13]. It is qualitatively different for the excitons in the biomolecular environment. Here,  $\hbar\omega_c$  is typically of the order of  $\sim 2 - 8$  meV, while the Förster coupling constants can range from  $\hbar\Delta \sim 0.2$  meV–100 meV [5, 11]. Hence, the bath responds slower than the dynamics of the excitons evolves, and non-Markovian effects become dominant. Coherent oscillations in a strongly damped two-state system with  $\alpha > 1$  and  $\Delta \gtrsim \omega_c$  have been found using quantum Monte Carlo simulations [14, 15] and by applying the numerical renormalization group [16].

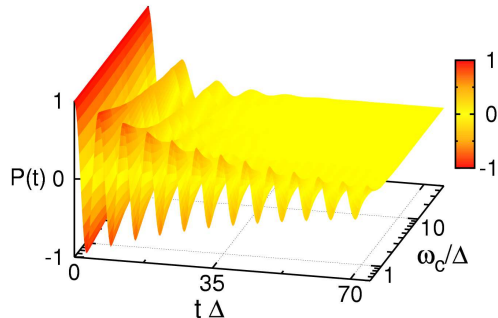


Figure 1: Population difference  $P(t)$  for a single chromophore pair and full cross-over from a Markovian to a non-Markovian bath. Parameters are  $k_B T = 0.1\hbar\Delta$ , and  $\alpha = 0.1$ .

### 3. Population dynamics of a single chromophore pair

Here, we use the quasiadiabatic path-integral (QUAPI) [6, 7, 8] to calculate the population difference  $P(t) = \langle \sigma_z \rangle_t$  [10] in the single pair. We choose  $P(0) = 1$ . Figure 1 shows the results for  $\alpha = 0.1$  (parameters correspond to *measured* values summarized in Ref. [5]).  $P(t)$  decays with time in an oscillatory way. The decay occurs faster for large  $\omega_c$  while for small  $\omega_c$ , the slow bath sustains more coherent oscillations. In general, for smaller  $\omega_c$  the spectral weight of the bath modes around the system frequency  $\Delta$  is suppressed and the decohering influence is reduced, yielding prolonged coherence. In fact, choosing  $\alpha = 0.1, \omega_c = 0.1\Delta$  (consistent with [1]), we find a coherence time of 1 ps which agrees well with the measured value of at least 660 fs [1], given the complexity of the setup. In passing, we note that we have compared with the Born-Markov result [10] for  $P(t)$  for small  $\omega_c$  and found strong disagreement, as expected (not shown).

### 4. Model for two coupled chromophore pairs

Next, we address entanglement between two chromophore pairs under the influence of a slow bath. We consider two equal pairs described by  $\sigma_{x/z,i}$ , coupled by an interpair Förster interaction  $J$  and coupled to a harmonic bath. The total Hamiltonian reads

$$H_2 = \sum_{i=1,2} \frac{\hbar\Delta}{2} \sigma_{x,i} + \hbar J (\sigma_{x,1} \sigma_{x,2} + \sigma_{y,1} \sigma_{y,2}) \quad (2)$$

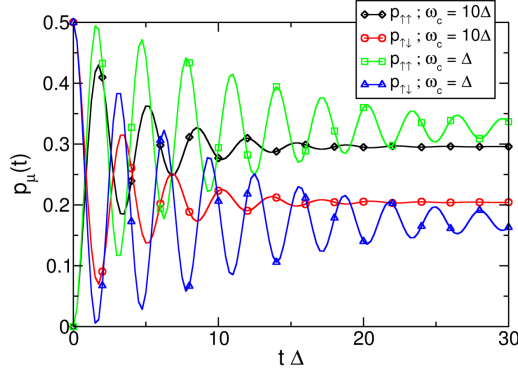


Figure 2: Time evolution of the populations  $p_\mu(t)$  for two coupled chromophore pairs for a slow ( $\omega_c = \Delta$ ) and a fast ( $\omega_c = 10\Delta$ ) bath, for  $k_B T = 0.1\hbar\Delta$ ,  $\alpha = 0.1$ , and  $J = 0.1\Delta$ .

$$+\frac{\hbar}{2}(\sigma_{z,1} + \sigma_{z,2}) \sum_{\kappa} c_{\kappa}(b_{\kappa}^{\dagger} + b_{\kappa}) + \sum_{\kappa} \hbar\omega_{\kappa} b_{\kappa}^{\dagger} b_{\kappa},$$

whose basis refers to the states  $\{|\uparrow_1\rangle = |e_1g_2\rangle, |\downarrow_1\rangle = |g_1e_2\rangle, |\uparrow_2\rangle = |e_3g_4\rangle, |\downarrow_2\rangle = |g_3e_4\rangle\}$ . As before, the bath spectral density follows from a Debye dielectric model, again yielding the Ohmic form. The time-dependent reduced density matrix  $\rho(t)$  is computed using an adapted QUAPI scheme. Figure 2 shows the time-evolution of the populations  $p_{\uparrow\uparrow}(t) = p_{\downarrow\downarrow}(t)$  and  $p_{\uparrow\downarrow}(t) = p_{\downarrow\uparrow}(t)$  of the four basis states for different values of  $\omega_c$  for the initial preparation  $|\psi_0\rangle = (|\uparrow_1\downarrow_2\rangle + |\downarrow_1\uparrow_2\rangle)/\sqrt{2}$ . After a transient oscillatory behavior, the stationary equilibrium values are reached. The corresponding decay occurs on shorter times for large  $\omega_c$ , i.e., fast baths, compared to the rather slow decay for small  $\omega_c$ .

## 5. Entanglement of two chromophore pairs

To quantify the two-pair quantum correlations, we study the entanglement along the negativity  $N(t) = \max\{0, -2\zeta_{\min}(t)\}$  [17, 18], where  $\zeta_{\min}(t)$  denotes the smallest eigenvalue of the partially transposed reduced density operator with the matrix elements  $\rho_{m\mu,n\nu}^{T_2} = \rho_{n\mu,m\nu}$ . A separable state has  $N = 0$ , while for a maximally entangled state,  $N = 1$ .

Figure 3(a) shows  $N(t)$  for two values  $\omega_c = \Delta$ , and  $\omega_c = 50\Delta$ , for the maximally entangled initial state  $|\psi_0\rangle$ . Starting from  $N(0) = 1$  we observe a decay to zero with small oscillations superimposed. For the Markovian bath

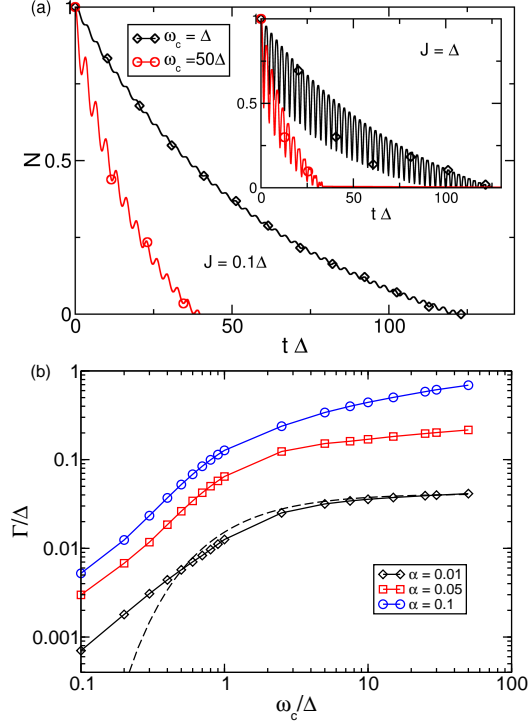


Figure 3: (a) Time evolution of the negativity  $N(t)$  for the cut-off  $\omega_c = \Delta$  (black) and  $\omega_c = 50\Delta$  (red) for  $\alpha = 0.01$  and for  $J = 0.1\Delta$  (main) and  $J = \Delta$  (inset). Moreover,  $k_B T = 0.1\hbar\Delta$ . (b) Decay constant  $\Gamma$  as a function of the cut-off  $\omega_c$  for different values of  $\alpha$  (symbols with solid lines) for  $k_B T = 0.1\hbar\Delta$ ,  $J = 0.1\Delta$ . Dashed line: Corresponding one-phonon result  $\Gamma = \Gamma_0 e^{-\Delta/\omega_c}$ , where the proportionality constant  $\Gamma_0 = 0.041\Delta$  has been obtained from a fit to the three data points  $\omega_c = 25\Delta, 30\Delta, 50\Delta$ .

$\omega_c = 50\Delta$ , the decay occurs faster than for the non-Markovian bath  $\omega_c = \Delta$ , indicating that entanglement survives on a longer time scale for the slow bath. For a larger interpair coupling  $J = \Delta$ , the superimposed oscillations are more pronounced (Fig. 3(a) inset) which is due to constructive interference of the transitions within the chromophore. For a quantitative picture, we fit an exponential  $N(t) = N_0 \exp(-\Gamma t) + N_1$  with a constant  $\Gamma$  which contains the influence of the bath. Figure 3(b) shows the dependence of  $\Gamma$  on  $\omega_c$ . Clearly,  $\Gamma$  strongly decreases for small  $\omega_c$ , while for large  $\omega_c$ , the decay rate saturates to a constant value. The dependence of  $\Gamma$  on  $\omega_c$  is more pronounced for larger values of  $\alpha$ . This observation indicates that entanglement could be at least as robust in biomolecular systems as in other macroscopic condensed-

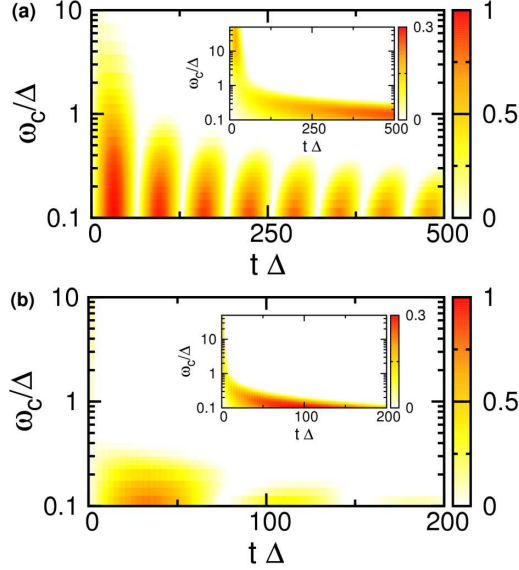


Figure 4: (a) Negativity  $N(t)$  as a function of  $\omega_c$  for  $J = 0.1\Delta$  (main) and  $J = 0$  (inset), for  $\alpha = 0.01$  and  $k_B T = 0.1\hbar\Delta$ . (b) Same as in (a), but for the strong coupling case  $\alpha = 0.1$ .

matter devices [13] which display quantum coherent behavior. We note that this tendency is already captured by the result of a one-phonon perturbative analysis, i.e., in second order perturbation theory. It would predict that for  $\omega_c \leq \Delta$  no bath modes for efficient one-phonon processes are available and  $\Gamma \propto G(\Delta) \propto e^{-\Delta/\omega_c}$ . A fit to the data points in the region of large  $\omega_c$  is shown by the dashed line in Fig. 3(b) for  $\alpha = 0.01$ . Clearly, when  $\omega_c \leq \Delta$ , multiphonon contributions become significant. This is even more pronounced for larger  $\alpha$  (not shown).

To study the cross-over between fast and slow baths, we show  $N(t)$  for varying  $\omega_c$  in Fig. 4 for the initial state  $|\psi_1\rangle = |\uparrow_1\uparrow_2\rangle$ . Figure 4(a) shows the result for  $J = 0.1\Delta$ . The entanglement is rather quickly destroyed in the regime  $\omega_c \gg \Delta$ . On the other hand, we find a regular oscillatory decay for  $0.1\Delta \lesssim \omega_c \lesssim \Delta$ . In this regime, complete entanglement disappearance and revivals alternate. The time scale of the entanglement oscillations is given by  $2\pi/J$ . The constructive role of a slow bath is further illustrated in the inset of Fig. 4(a), where  $N(t)$  is shown for  $J = 0$ . In fact, in the regime  $\omega_c < \Delta$ , we find that entanglement between the two pairs is generated by their common

interaction with a slow bath. Most interestingly, for  $\omega_c = 0.1\Delta$ ,  $N(t)$  steadily grows even over rather long times up to  $t\Delta = 500$ . In view of the single-pair results described above, this seems counterintuitive since for small  $\omega_c$ , a reduced influence of the bath modes would be expected. However, in this regime, the bath is rather efficient in generating entanglement. This feature survives even for larger values of  $\alpha$ , see Fig. 4(b). The oscillatory behavior of the entanglement generation still occurs for  $J = 0.1\Delta$ , where  $N(t)$  assumes all values between zero and one. The bath-induced destruction happens here earlier due to the large  $\alpha$ . Entanglement is also produced when  $J = 0$ , see inset of Fig. 4(b), for  $0.1\Delta \lesssim \omega_c \lesssim \Delta$ . Also here,  $N(t)$  can even reach the maximal value at intermediate times.

The generation of entanglement can be qualitatively understood by performing a polaron-like transformation  $U = \exp[i(\sigma_{z,1} + \sigma_{z,2})p/2]$  with  $p = \sum_{\kappa} ic_{\kappa}(b_{\kappa}^{\dagger} - b_{\kappa})$ . Setting  $J = 0$  and assuming that the two qubits are spatially close enough, the resulting Hamiltonian  $\tilde{H}_2 = U^{\dagger}H_2U$  acquires an effective direct coupling  $\tilde{H}_{2,\text{int}} = \hbar J_{\text{eff}}\sigma_{z,1}\sigma_{z,2}$  with  $J_{\text{eff}} = -\alpha\omega_c/8 \sim E_r$  (note that restrictions to the applicability of  $U$  apply. Details will be published elsewhere). Then, the long-wave length bath modes are efficient in generating coherent coupling, and thus entanglement. Its dynamical generation occurs on a time scale  $1/J_{\text{eff}}$ , see insets of Fig. 4. On the other hand, damping destroys coherence on a time scale  $\Gamma$  related to  $\omega_c$ , see Fig. 3, i.e., for large  $\omega_c$ , damping beats entanglement generation.

So far, we have studied not so high temperatures, similar to the experimental conditions in Refs. [1, 2]. However, in Fig. 5(a) (main) we plot  $N(t)$  for varying  $\omega_c$ , for  $k_B T = \hbar\Delta$ , for the initial state  $|\psi_1\rangle$ . We still find large entanglement oscillations at short to intermediate times, for  $0.1\Delta \lesssim \omega_c \lesssim \Delta$  despite the rather large temperature: this is an outstanding hardware feature that could provide a useful resource for the artificial design of controlled, robust, and efficient biomolecular nanostructures for quantum information processing [19, 20, 21].

Furthermore, we have varied the initial preparation to the state  $|\psi_2\rangle = a|\uparrow_1\downarrow_2\rangle + b|\downarrow_1\uparrow_2\rangle$  with  $a^2 + b^2 = 1$ . The inset of Fig. 5(a) shows  $N(t)$  for varying  $a^2$  and  $J = 0.1\Delta$ .  $|\psi_2\rangle$  is maximally entangled for  $a^2 = 1/2$ , for which  $N(t)$  decays monotonously with time, while away from this region the negativity again shows collapses and revivals. For the borders  $a^2 \rightarrow 0, 1$ ,  $|\psi_2\rangle$  is a separable state, but entanglement is rather quickly generated with time before it finally dies out. Robust entanglement thus depends on the initial preparation and is favored by the choice of initially separable (or weakly



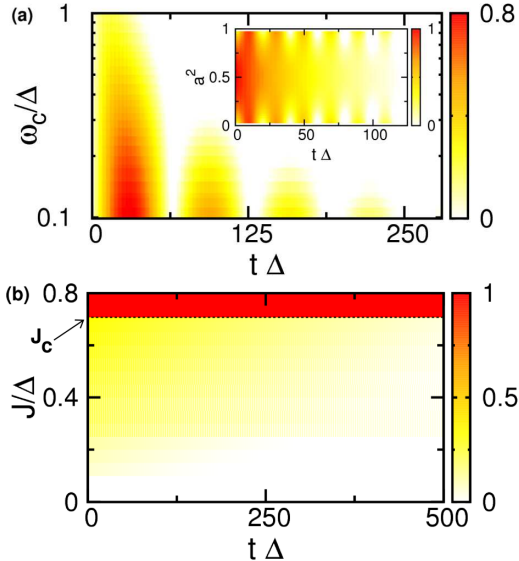


Figure 5: (a) Negativity  $N(t)$  for varying  $\omega_c$ ;  $J = 0.1\Delta$ ,  $\alpha = 0.01$  and  $k_B T = \hbar\Delta$  (Main). Inset:  $N(t)$  for different initial preparations  $|\psi_2\rangle = a|\uparrow_1\downarrow_2\rangle + b|\downarrow_1\uparrow_2\rangle$ , for  $J = 0.1\Delta$ ,  $\alpha = 0.01$ ,  $k_B T = 0.1\hbar\Delta$ , and  $\omega_c = \Delta$ . (b)  $N(t)$  for varying  $J$ ;  $\alpha = 0.01$ ,  $k_B T = 0.1\hbar\Delta$ ,  $\omega_c = 0.1\Delta$ .  $J_c = 1/\sqrt{2}$  marks the border above which the initial ground state belongs to a DFS.

entangled) states.

Finally, we analyze the dependence on the interpair coupling  $J$ . The negativity  $N(t)$  is shown in Fig. 5(b) for varying  $J$  for the respective ground state as the initial preparation. From Eq. (2) it follows that a critical value  $J_c = 1/\sqrt{2}$  exists such that for  $J \geq J_c$ , the state  $|\psi_g\rangle = (|\uparrow_1\downarrow_2\rangle - |\downarrow_1\uparrow_2\rangle)/\sqrt{2}$  is the two-pair groundstate, which, however, belongs to a decoherence-free subspace (DFS) of  $H_2$  [22]. Hence,  $N(t)$  remains constantly maximal. For  $J < J_c$ , the ground state has some weight outside of the DFS and hence suffers from decoherence.

We emphasize that we have formulated our approach in quantum statistical terms. It directly involves the reduced density operator which describes mixed ensemble states. Thus, the entanglement dynamics reported here manifests itself in a statistical many-particle ensemble and, hence, would appropriately allow the design and implementation of robust biomolecular entanglement proof-of-principle experiments with current technology.

## 6. Conclusions

In this Letter, we have shown that non-Markovian effects are vital for the correct description of the entanglement dynamics of biomolecular excitonic qubits. Recent results obtained from a reduced hierarchy equation approach [23] are within the lines of our findings. While our QUAPI technique yields numerically exact results, the approach developed in [23] allows to include non-Markovian corrections only up to a certain extent. In either case, the results yield that the validity of the Born-Markov approximation for the treatment of slow protein-solvent environments in photosynthetic complexes [24] is questionable, even in the regime of high temperature; see, e.g., our Fig. 5.

Our results are relevant to molecular architectures [25, 26] and ultrafast processes [27]. They could prove crucial in the design of artificial light harvesters for robust biomolecular entanglement, with enhanced energy transfer rates [28] for the control [21] of quantum bits. Most importantly, our predictions could be tested with currently available experimental techniques [1, 2, 3, 4]. For instance, advanced ultrafast spectroscopy techniques allow to measure the time dependence of the elements of the two-particle reduced density matrix from which an entanglement measure can be derived straightforwardly. Similarly, such an experiment would give direct insight into the interpair coupling strength which can directly be derived from the oscillation period of the entanglement measure. It should also be possible to prepare desired initial states. A further crucial topic is the behavior of this effect at higher temperature which can be experimentally doable. We hope that our results can be experimentally demonstrated in the near future.

### A. Acknowledgment

We acknowledge support by the DFG SPP 1243, COLCIENCIAS grs. 1106-14-17903, 1106-452-21296, DAAD PROCOL, and the Excellence Initiative of the German Federal and State Governments and CPU time from the ZIM in Düsseldorf.

### References

- [1] G.S. Engel, T.R. Calhoun, E.L. Read, T.-K. Ahn, T. Mancal, Y.-C. Cheng, R.E. Blankenship, G.R. Fleming, *Nature* **446** (2007) 782.

- [2] H. Lee, Y.-C. Cheng, G. R. Fleming, *Science* **316** (2007) 1462.
- [3] T. Brixner, J. Stenger, H.M. Vaswani, M. Cho, R.E. Blankenship, G.R. Fleming, *Nature* **434** (2005) 625.
- [4] J. L. Herek, W. Wohlleben, R. J. Cogdell, D. Zeidler, M. Motzkus, *Nature* **417** (2002) 533.
- [5] J. Gilmore, R. McKenzie, *Chem. Phys. Lett.* **421** (2006) 266.
- [6] N. Makri, *J. Math. Phys.* **36** (1995) 2430.
- [7] N. Makri, E. Sim, D. Makarov, M. Topaler, *Proc. Natl. Acad. Sci. USA* **93** (1996) 3926.
- [8] M. Thorwart, P. Reimann, P. Jung, R. F. Fox, *Chem. Phys.* **235** (1998) 61.
- [9] B. Bellomo, R. Lo Franco, G. Compagno, *Phys. Rev. Lett.* **99** (2007) 160502.
- [10] U. Weiss, *Quantum Dissipative Systems*, 3rd ed., World Scientific, Singapore, 2008.
- [11] J. Gilmore, R. McKenzie, *J. Phys. Chem. A* **112** (2008) 2162.
- [12] V. May, O. Kühn, *Charge and energy transfer dynamics in molecular systems*, Wiley, Berlin, 2001.
- [13] Y. Makhlin, G. Schön, A. Shnirman, *Rev. Mod. Phys.* **73** (2001) 357.
- [14] R. Egger, C. H. Mak, *Phys. Rev. B* **50** (1994) 15210.
- [15] L. Mühlbacher, R. Egger, *J. Chem. Phys.* **118** (2003) 179.
- [16] R. Bulla, H.-J. Lee, N.-H. Tong, M. Vojta, *Phys. Rev. B* **71** (2005) 045122.
- [17] A. Peres, *Phys. Rev. Lett.* **77** (1996) 1413.
- [18] M. Horodecki, P. Horodecki, R. Horodecki, *Phys. Lett. A* **223** (1996) 1.
- [19] M. Kroutvar, Y. Ducommun, D. Heiss, M. Bichler, D. Schuh, G. Abstreiter, J. Finley, *Nature* **432** (2004) 81.

- [20] P. Rabl, D. DeMille, J. Doyle, M. Lukin, R. Schoelkopf, P. Zoller, Phys. Rev. Lett. **97** (2006) 033003.
- [21] M. Thorwart, P. Hänggi, Phys. Rev. A **65** (2002) 012309.
- [22] J. H. Reina, L. Quiroga, N. F. Johnson, Phys. Rev. A **65** (2002) 032326.
- [23] A. Ishizaki, G. R. Fleming, J. Chem. Phys. **130** (2009) 234111.
- [24] M. Mohseni, P. Rebentrost, S. Lloyd, and A. Aspuru-Guzik, J. Chem. Phys. **129** (2008) 174106.
- [25] S. A. Crooker, J. A. Hollingsworth, S. Tretiak, V. I. Klimov, Phys. Rev. Lett. **89** (2002) 186802.
- [26] J. H. Reina, R.G. Beausoleil, T.P. Spiller, W.J. Munro, Phys. Rev. Lett. **93** (2004) 250501.
- [27] P. Agostini, L.F. DiMauro, Rep. Prog. Phys. **67** (2004) 813.
- [28] K. Becker, J.M. Lupton, J. Müller, A.L. Rogach, D.V. Talapin, H. Weller, J. Feldmann, Nature Mater. **5** (2006) 777.